Percolation of light through whispering gallery modes in 3D lattices of coupled microspheres

Vasily N. Astratov and Shashanka P. Ashili

Department of Physics and Optical Science, Center for Optoelectronics and Optical Communications, University of North Carolina at Charlotte, Charlotte, NC 28223-0001
astratov@uncc.edu

Abstract: Using techniques of flow-assisted self-assembly we synthesized three-dimensional (3D) lattices of dye-doped fluorescent (FL) 5 μm polystyrene spheres with 3% size dispersion with well controlled thickness from one monolayer up to 43 monolayers. In FL transmission spectra of such lattices we observed signatures of coupling between multiple spheres with nearly resonant whispering gallery modes (WGMs). These include (i) splitting of the WGM-related peaks with the magnitude 4.0-5.3 nm at the average wavelength 535 nm, (ii) pump dependence of FL transmission showing that the splitting is seen only above the threshold for lasing WGMs, and (iii) anomalously high transmission at the WGM peak wavelengths compared to the background for samples with thickness around 25 μm. We propose a qualitative interpretation of the observed WGM transport based on an analogy with percolation theory where the sites of the lattice (spheres) are connected with optical "bonds" which are present with probability depending on the spheres' size dispersion. We predict that the WGM percolation threshold should be achievable in close packed 3D lattices formed by cavities with ~10^3 quality factors of WGMs and with ~1% size dispersion. Such systems can be used for developing next generation of resonant sensors and arrayed-resonator light emitting devices.

OCIS codes: (230.5750) Resonators; (230.4555) Coupled resonators; (350.3950) Micro-Optics.

References and links

1. P. W. Anderson, "Absence of diffusion in certain random lattices", Phys. Rev. **109**, 1492-1505 (1958).
2. S. John, "Electromagnetic absorption in a disordered medium near a photon mobility edge," Phys. Rev. Lett. **53**, 2169-2172 (1984).
3. M. Stoytchev and A. Z. Genack, "Measurement of the probability distribution of total transmission in random waveguides," Phys. Rev. Lett. **79**, 309-312 (1997).
4. P. W. Brouwer, "Transmission through a many-channel random waveguide with absorption," Phys. Rev. B **57**, 10526-10536 (1998).
5. D. S. Wiersma, P. Bartolini, A. Lagendijk, and R. Righini, "Localization of light in a disordered medium," Nature **390**, 671-673 (1997).
6. M. Störzer, P. Gross, C. M. Aeggerter, and G. Maret, "Observation of the critical regime near Anderson localization of light," Phys. Rev. Lett. **96**, 063904 (2006).
7. B. E. Little, S. T. Chu, H. A. Haus, J. Foresi, and J.-P. Laine, "Microring resonator channel dropping filters," J. Lightwave Technol. **15**, 998-1005 (1997).
8. A. Yariv, Y. Xu, R. K. Lee, and A. Scherer, "Coupled-resonator optical waveguide: a proposal and analysis," Opt. Lett. **24**, 711-713 (1999).
9. N. Stefanou, A. Modinos, "Impurity bands in photonic insulators," Phys. Rev. B, **57**, 12127-12133 (1998).
10. T. Mukaiyama, K. Takeda, H. Miyazaki, Y. Jimba, and M. Kuwata-Gonokami, "Tight-binding photonic molecule modes of resonant bispheres," Phys. Rev. Lett. **82**, 4623-4626 (1999).
11. M.D. Barnes, S.M. Mahurin, A. Mehta, B.G. Sumpter, and D.W. Noid, "Three-Dimensional photonic "molecules" from sequentially attached polymer-blend microparticles," Phys. Rev. Lett. **88**, 015508 (2002).
12. Y. Hara, T. Mukaiyama, K. Takeda, and M. Kuwata-Gonokami, "Photonic molecule lasing," Opt. Lett. **28**, 2437-2439 (2003).
13. H. Guo, H. Chen, P. Ni, Q. Zhang, B. Cheng, and D. Zhang, "Transmission modulation in the passband of polystyrene photonic crystals," Appl. Phys. Lett. **82**, 373-375 (2003).

#88612 - $15.00 USD Received 15 Oct 2007; revised 3 Dec 2007; accepted 4 Dec 2007; published 10 Dec 2007

14. V. N. Astratov, J. P. Franchak, and S. P. Ashili, "Optical coupling and transport phenomena in chains of spherical dielectric microresonators with size disorder," Appl. Phys. Lett. **85**, 5508-5510 (2004).
15. Y. P. Rakovich, J. F. Donegan, M. Gerlach, A. L. Bradley, T. M. Connolly, J. J. Boland, N. Gaponik, and A. Rogach, "Fine structure of coupled optical modes in photonic molecules," Phys. Rev. A **70**, 051801(R) (2004).
16. Y. Hara, T. Mukaiyama, K. Takeda, and M. Kuwata-Gonokami, "Heavy photon states in photonic chains of resonantly coupled cavities with supermonodispersive microspheres," Phys. Rev. Lett. **94**, 203905 (2005).
17. B. M. Möller, U. Woggon, and M. V. Artemyev, "Coupled-resonator optical waveguides doped with nanocrystals," Opt. Lett. **30**, 2116-2118 (2005).
18. A. V. Kanaev, V. N. Astratov, and W. Cai, "Optical coupling at a distance between detuned spherical cavities," Appl. Phys. Lett. **88**, 111111 (2006).
19. S. P. Ashili, V. N. Astratov, and E. C. H. Sykes, "The effects of inter-cavity separation on optical coupling in dielectric bispheres," Opt. Express **14**, 9460-9466 (2006).
20. B. M. Möller, U. Woggon, and M. V. Artemyev, "Bloch modes and disorder phenomena in coupled resonator chains," Phys. Rev. B **75**, 245327 (2007).
21. S. Deng, W. Cai, and V. N. Astratov, "Numerical study of light propagation via whispering gallery modes in microcylinder coupled resonator optical waveguides," Opt. Express **12**, 6468-6480 (2004).
22. S. V. Boriskina, "Theoretical prediction of a dramatic Q-factor enhancement and degeneracy removal of whispering gallery modes in symmetrical photonic molecules," Opt. Lett. **31**, 338-340 (2006).
23. J.E. Heebner, R. W. Boyd, and Q. H. Park, "SCISSOR solitons and other novel propagation effects in microresonator-midified waveguides," J. Opt. Soc. Am. B **19**, 722-731 (2002).
24. A. Melloni, F. Morichetti, and M. Martinelli, "Linear and nonlinear pulse propagation in coupled resonator slow-wave optical structures," Opt. Quantum Electron. **35**, 365-379 (2003).
25. B. E. Little, S. T. Chu, P. P. Absil, J. V. Hryniewicz, F. G. Johnson, F. Seiferth, D. Gill, V. Van, O. King, and M. Trakalo, "Very high-order microring resonator filters for WDM applications," IEEE Photon. Technol. Lett. **16**, 2263-2265 (2004).
26. J. K. S. Poon, L. Zhu, G. A. DeRose, and A. Yariv, "Transmission and group delay of microring coupled-resonator optical waveguides," Opt. Lett. **31**, 456-458 (2006).
27. F. Xia, L. Sekaric, and Yu. A. Vlasov, "Ultra-compact optical buffers on a silicon chip," Nature Photon. **1**, 65-71 (2007).
28. A. B. Matsko and V. S. Ilchenko, "Optical resonators with whispering-gallery modes – part I: basics," IEEE J. Sel. Top. Quantum Electron. **12**, 3-14 (2006).
29. V. S. Ilchenko and A. B. Matsko, "Optical resonators with whispering-gallery modes – part II: applications," IEEE J. Sel. Top. Quantum Electron. **12**, 15-32 (2006).
30. S. Mookherjea and A. Oh, "Effect of disorder on slow light velocity in optical slow-wave structures," Opt. Lett. **32**, 289-291 (2007).
31. R. Albert and A.-L. Barabasi, "Statistical mechanics of complex networks," Rev. Mod. Phys. **74**, 47-97 (2002).
32. C. D. Lorenz and R. M. Ziff, "Precise determination of the bond percolation thresholds and finite-size scaling corrections for the sc, fcc, and fcc lattices," Phys. Rev. E **57**, 230-236 (1998).
33. M. F.Sykes and J. W. Essam, "Exact critical percolation probabilities for site and bond problems in two dimensions," J. of Math. Phys. (N.Y.) **5**, 1117-1127 (1964).
34. B. Gates, D. Qin, and Y. Xia, "Assembly of nanoparticles into opaline structures over large areas," Adv. Mater. **11**, 466-469 (1999).
35. V. N. Astratov, A. M. Adawi, S. Fricker, M. S. Skolnick, D. M. Whittaker, and P. N. Pusey, "Interplay of order and disorder in the optical properties of opal photonic crystals," Phys. Rev. B **66**, 165215 (2002).
36. Z. Chen, A. Taflove, and V. Backman, "Photonic nanojet enhancement of backscattering of light by nanoparticles: a potential novel visible-light ultramicroscopy technique," Opt. Express **12**,1214-1220 (2004).
37. A. M. Kapitonov and V. N. Astratov, "Observation of nanojet-induced modes with small propagation losses in chains of coupled spherical cavities," Opt. Lett. **32**, 409-411 (2007).
38. V. S. Ilchenko, P. S. Volkov, V. L. Velichansky, F. Treussart, V. Lefèvre-Seguin, J.-M. Raimond, and S. Haroche, "Strain-tunable high-Q optical microsphere resonator," Opt. Comm. **145**, 86-90 (1998).
39. N. Le Thomas, U. Woggon, W. Langbein, and M. V. Artemyev, "Effect of a dielectric substrate on whispering-gallery-mode sensors," J. Opt. Soc. Am. B **23**, 2361-2365 (2006).
40. H. C. van de Hulst, *Light scattering by small particles* (Dover Publications, Inc., New York, 1981).
41. M. Sumetsky and B. J. Eggleton, "Modeling and optimization of complex photonic resonant cavity circuits," Opt. Express **11**, 381-391 (2003).
42. J. E. Heebner, P. Chak, S. Pereira, J. E. Sipe, and R. W. Boyd, "Distributed and localized feedback in microresonator sequences for linear and nonlinear optics," J. Opt. Soc. Am. B **21**, 1818-1832 (2004).
43. M. Sumetsky, "Modelling of complicated nanometer resonant tunneling devices with quantum dots," J. Phys.: Condens. Matter **3**, 2651-2664 (1991).

#88612 - $15.00 USD Received 15 Oct 2007; revised 3 Dec 2007; accepted 4 Dec 2007; published 10 Dec 2007

1. Introduction

Traditionally, light localization [1,2] and various interference effects [3,4] have been studied in structures formed by scatterers, such as powders [5,6] of dielectric or semiconductor materials, with dimensions comparable to the wavelength of light. Recent proposals of high order optical filters [7] and coupled resonator optical waveguides (CROW) [8,9] stimulated a strong interest to the optical transport mechanisms in mesoscopic systems formed by spherical [10-20], cylindrical [21,22], or ring [23-27] resonators with the typical sizes in the order of several wavelengths. The light is tightly confined in such cavities due to whispering gallery modes (WGMs) [28,29] with extremely high quality resonances ($Q>10^3$ for 4 μm spheres and up to ~10^9 for submillimeter spheres). The light transport from cavity to cavity is due to evanescent coupling of WGMs to neighboring resonators.

It should be noted that disorder plays a fundamental role in the slow light [30] properties and in the spectral transmission characteristics of CROW structures. One of the problems is the scattering losses caused by size and shape variations of the cavities which lead to random energy detuning of their WGM eigenstates. The commercial suspensions of microspheres have inevitable ~1% size dispersion. By using numerical modeling it was demonstrated [18] that the size-mismatched spherical cavities can be coupled due to excitation of the quasi-WGMs with distorted shape. This mechanism provides a limited efficiency of coupling (~0.1-0.2) between cavities with strongly detuned WGM eigenstantes. Such WGM-related coupling and transport phenomena were observed in size-mismatched bispheres [19] and in chains [14,20] of spheres with the size disorder.

In the case of microspheres, the cavities can be micromanipulated and sorted individually which opens a possibility to select much more uniform resonators [10,12,15-17] on the basis of spectroscopic characterization of their WGM peak positions. These techniques allow selecting spheres with the size uniformity ~0.03%. The band structure effects due to tight-binding model [16] as well as normal mode splitting effects [10,15,17] have been observed in supermonodispersive spheres. However the sorting of large numbers of microspheres ($Q>10^4$) with overlapping positions of WGM peaks still remains a challenging problem.

The optical transport in disordered mesoscopic systems of coupled cavities can be compared with the case of random waveguides [3,4] formed by wavelength scale scatterers. In random waveguides the importance of interference phenomena such as strong fluctuations in the transmitted intensity through a disordered sample is determined by the ratio Nl/d, where N is the number of transverse propagating channels in the waveguide, d its length and l is the elastic mean free path. To observe strong fluctuations, it is important to achieve as low values of Nl/d as possible [4]. In coupled cavities, the light effectively propagates along the lines connecting close neighbors forming a network. Changing direction or "scattering" effectively takes place at the touching points between the cavities, so the elastic mean free path l can be associated with the size of the cavities. In the case of large scale 2D or 3D networks of coupled resonators, the number of transverse paths N can be extremely high meaning that the interference phenomena can be averaged.

It is interesting to note that the optical transport in systems of coupled cavities can be considered by analogy with the "bond percolation" problem [31,32] in percolation theory. The cavities arranged as a lattice are connected at the WGM wavelengths with optical "bonds" which are present with probability p depending on the cavities' size dispersion (assuming $p\approx1$ in the resonant case). At small p only a few bonds are present, thus only small clusters of sites (spheres) can form, but at a critical probability p_c, called the percolation threshold [31,32], a giant cluster appears spanning the entire network. The bond percolation threshold for 2D triangular lattice is p_c= 0.3472963…[33], whereas for 3D face-centered-cubic (fcc) lattice it is only p_c=0.1201635 [32]. It should be noted that in the case of WGM coupling in 3D case the multiple spheres can be preferably connected in the "atomic" plans of such fcc lattice that should result in anisotropic properties and higher than p_c=0.1201635 thresholds of such percolative transport, however still the WGM transport in a 3D lattice of spheres is expected

#88612 - $15.00 USD Received 15 Oct 2007; revised 3 Dec 2007; accepted 4 Dec 2007; published 10 Dec 2007

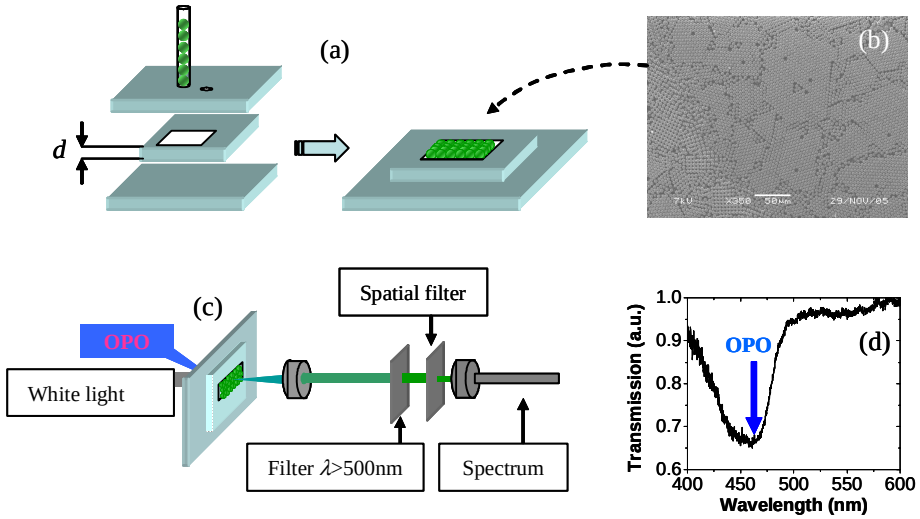

Fig. 1. (a) Sketch of the cell for the hydrodynamic flow-assisted self-assembly of microspheres, (b) SEM image of the top surface of the sample showing its polycrystalline structure, (c) experimental set up, (d) single dye-doped sphere transmission spectrum.

to be much more robust to the presence of disorder compared to that in 1D chains or 2D arrays of cavities.

In this paper we study the WGM transport properties of 3D lattices of closely packed fluorescent (FL) microspheres with the mean diameter 5 μm and 3% size dispersion. Using a technique of hydrodynamic flow-assisted self-assembly [34], we fabricated a set of samples with the thickness varying from one monolayer up to 43 monolayers. Using techniques of local photoexcitation we observed splitting of WGM-related FL transmission peaks above certain pumping threshold. We also observed an unusual dependence of the WGM-related transmitted intensity on the thickness of the structure. We explain these results by the presence of localized clusters or configurations of nearly uniform spheres inside our 3D structures well connected at the WGM wavelengths.

2. Structures and experimental setup

The 3D close-packed structures formed by 5 μm dye-doped (Green FL, Duke Scientific Corp.) polystyrene microspheres with ~3% size dispersion were synthesized by the technique [34] of hydrodynamic flow-assisted self-assembly. As shown in Fig. 1(a) the suspension of spheres was injected into a cell fabricated by sandwiching a mylar film with a rectangular hole between two glass substrates. Submicron scratches fabricated on the surface of the mylar film allowed the liquid to leak out whereas the spheres were trapped inside the cell. The growth of the close-packed structure with ~1 cm^2 area was accelerated under continuous sonication. The thickness (d) of this structure was controlled by the mylar films in 5 – 177 μm range.

Although polycrystalline, such samples have fcc domains with typical dimensions greater than 50 μm, as illustrated in Fig. 1(b). The triangular packing of spheres in Fig. 1(b) represents [35] domains with (111) planes parallel to the surface. About 90% of the total area of the sample was shown to contain domains with the (111) planes parallel to its surface.

White light illumination was used for imaging different areas of the samples and for taking transmission spectra of individual spheres, as illustrated in Figs. 1(c,d). The pronounced dip, around 467 nm, in Fig. 1(d) is due to the absorption of dye molecules doped throughout the entire volume of microspheres. It should be noted that the illumination of the microspheres with plane waves leads to the formation of "photonic nanojets" [36] at the back side of spheres and to the formation of nanojet-induced modes [37] in cavity chains. However the plane wave illumination is poorly coupled to WGMs in spheres.

#88612 - $15.00 USD Received 15 Oct 2007; revised 3 Dec 2007; accepted 4 Dec 2007; published 10 Dec 2007

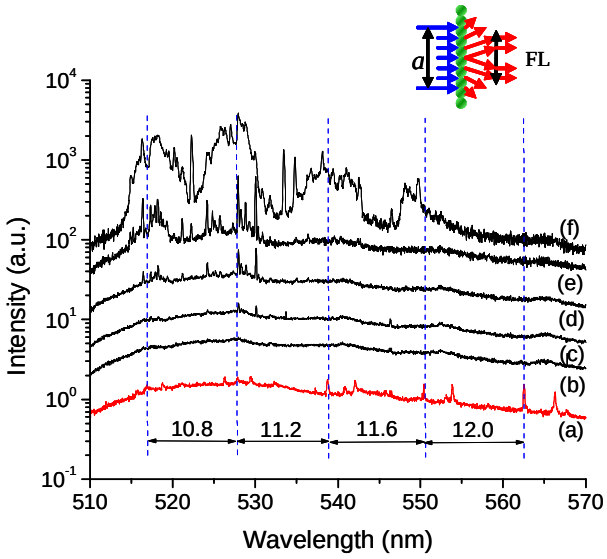

Fig. 2. (a) Single 5μm sphere emission spectrum below the threshold for lasing WGMs and (b-f) emission spectra of a single monolayer of 5μm spheres collected as a function of average excitation intensity from 0.03 W/cm^2 to 100 W/cm^2. Inset illustrates geometry of excitation and collection of FL emission.

In order to study the transport of WGMs we created a localized FL source at one side of the sample by illuminating it with the focused beam from an optical parametric oscillator (OPO) system with 5ns pulses and repetition rate of 20Hz, tuned to the center of the absorption band of the dye (467 nm). The focused spot had a Gaussian intensity distribution at the sample with the half width a=30 μm leading to an excitation of about 30 spheres in the first monolayer. The attenuation length of the pump, due to absorption of the dye, can be estimated as l_a ~13 μm. Thus, in thick lattices (d>l_a) the FL source was confined near the illuminated surface of the structure. As shown in Fig. 1(c) the optical transport properties were studied by detecting FL transmission spectra from the opposite side of the sample. We used a 100× objective (NA=0.5) coupled to the spectrometer through a spatial filter selecting a ~10 μm circular area at the surface of the sample located opposite to the center of the excitation spot.

3. Experimental results and discussion

3.1. Pumping dependence of emission of a single monolayer

We first present in Fig. 2 the results of characterization of a single monolayer of microspheres. In this case the spheres are coupled laterally, and the effects of transport between the layers are not involved.

For comparison purposes Fig. 2(a) shows the low-intensity FL emission spectrum of a single isolated sphere demonstrating WGM peaks with 11-12 nm separations which is expected given the free spectral range of a 5 μm sphere. This spectrum was obtained by selecting the emission from a central area on the sphere equator using a spatial filter. Generally, the WGM resonances in spherical cavities [28,29] are characterized by their polarization (TE/TM) and by radial (n), angular (l), and azimuthal (m) numbers. In perfect spheres the WGM modes are 2l+1 fold degenerate in m. This degeneracy can be removed by deformations from the spherical shape [38]. The modes with n=1 (one antinode of the electromagnetic field in the radial direction) are most closely confined to the surface of the sphere, and they have highest Q-factors of their WGM resonances. The spectral resolution in Fig. 2 is limited by the spectrometer at ~0.2 nm level. Our measurements with higher spectral resolution showed that the sharpest peaks in Fig. 2(a) (corresponding to n=1) are characterized

#88612 - $15.00 USD Received 15 Oct 2007; revised 3 Dec 2007; accepted 4 Dec 2007; published 10 Dec 2007

with $Q = 4\times10^3$. It has been demonstrated [39] that such values of Q-factors are much smaller than that predicted by the Mie theory as a result of an inhomogeneous broadening due to the spheres shape deformations and as a consequence of a homogeneous broadening for modes with small azimuthal numbers m due to the tunneling to the substrate. The latter factor leads to highest Q factors for modes with $|m|\sim l$ located in the vicinity of equatorial plane of spheres.

The FL emission spectra of a single monolayer of microspheres are presented in Figs. 2(b-f) as a function of the average excitation intensity (I_{av}) from 0.03 W/cm^2 to 100 W/cm^2. The low excitation intensity spectra in Figs. 2(b,c) display a series of nearly equidistant broad and weakly pronounced maxima. These maxima appear due to the inhomogeneous broadening of the WGM peaks originating from multiple laterally coupled size-disordered cavities located within the excitation spot. The orientation of WGM orbits close to the equatorial plane favors coupling between adjacent cavities once they are assembled as a closed packed monolayer on the substrate. It should be noted however that due to large random detuning (~15 nm) between the uncoupled WGM eigenstates (caused by ~3% size disorder) such coupling is provided in an undercoupled regime with a limited (~0.1-0.2) coupling efficiency, as it was demonstrated by numerical modeling [18] for touching size-mismatched bispheres. The weak coupling between ~30 touching spheres located within the excitation spot results in a significant inhomogeneous broadening of the WGM-related maxima in the emission spectra detected from the central (10 μm) part of this spot.

These maxima are weak since up to a threshold of ~0.3 W/cm^2 corresponding to Fig. 2(d) only a few percent of the total spontaneous emission intensity is coupled to WGMs [12], and most of the FL intensity is emitted into radiative modes with a broad (510-570nm) spectrum. Above this threshold, however, the individual spheres start to operate as WGM microlasers. Lateral coupling of ~30 size-disordered WGM microlasers located within the excitation spot gives rise to very strong inhomogeneously broadened peaks in the emission spectrum of single monolayer, as illustrated in Fig. 2(f).

3.2. Pumping dependence of FL transmission of several monolayers thick structures

The spectra of FL transmission through the six monolayer thick structure with d=25.4 μm are presented in Fig. 3. Since the structure is strongly absorbing at the pump wavelength (467nm), and nearly transparent at the emission wavelengths at 510-570 nm, the transport of light from the illuminated side of the sample to the area of collection plays a key role in formation of FL transmission spectra.

There are two major mechanisms which can be involved in such transport. One is connected with nonresonant diffusive propagation of radiative modes emitted by the source spheres. Using traditional scattering terminology [40] this transport can be referred to as a scattering by large spherical particles ($x=2\pi a/\lambda>>1$, where a=2.5 μm is the radius of microsphere) with relatively small (0.59) index contrast. In this limit most of the light is transmitted through each sphere after two refractions without a significant inner reflection. In the case of plane wave illumination this leads to formation of photonic nanojets [36,37] due to the focusing effect produced by individual spheres. The second mechanism is connected with evanescent coupling [18] of WGMs. High pumping intensities strongly favor the latter mechanism since at highest powers almost 100% of the emission of the source spheres is provided into the WGM lasing modes as opposed to the radiative modes.

A series of the FL transmission spectra measured as a function of I_{av} is presented in Fig. 3. Up to a threshold of I_{av}~0.3 W/cm^2 corresponding to Fig. 3(c), the spectra display a set of nearly equidistant broad maxima similar to that in Figs. 2(b-c). However, at higher I_{av} each maximum is observed to transform into a double-peak structure with 4.0-5.3 nm splitting, as indicated by dashed lines in Fig. 3. Similar splitting at I_{av}>0.3 W/cm^2 was observed in all samples with thicknesses ranging from 9.1 μm (2 monolayers) up to 177 μm (43 monolayers). It is seen in Fig. 3 that the magnitude of splitting does not depend on the pumping intensity.

An inset of Fig. 3 shows the dependence of the FL transmission on the pump intensity for the peak at 529.3 nm (red line) and for the FL background at the same wavelength (blue line).

#88612 - $15.00 USD Received 15 Oct 2007; revised 3 Dec 2007; accepted 4 Dec 2007; published 10 Dec 2007

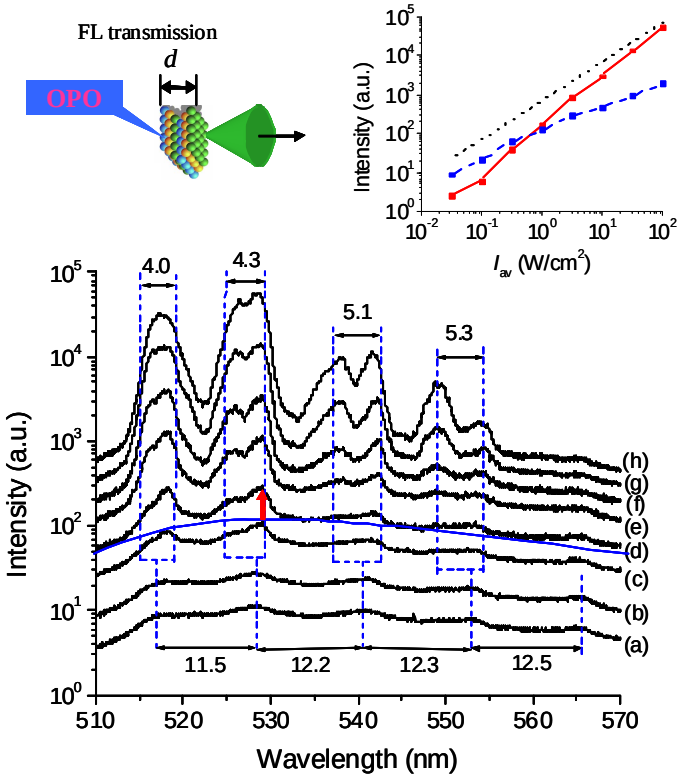

Fig. 3. FL transmission spectra of a six layer thick sample (d=25.4 μm) collected as a function of excitation intensity (I_{av}) from (a) 0.03 W/cm^2 to (h) 100 W/cm^2. (c-h) For I_{av}>0.3 W/cm^2 each maximum transforms into a double peak. Inset: pump dependence of the peak at 529.3 nm (red line), background emission (blue line) and a linear fit (black line).

To obtain the net output related to the WGM contribution, we subtracted the broad FL background that corresponds to the emission from dye molecules in the central regions of the cavities, as illustrated in the spectrum of Fig. 3(d). It is seen that the WGM contribution (red line) increases superlinearly with the pump whereas the FL background emission (blue line) behaves sublinearly, as illustrated by comparison with a linear fit (black line).

The observed formation of a double peak structure in the FL transmission spectra can be explained by the WGM coupling phenomena in clusters of touching cavities. Due to the 3% size disorder of cavities in our samples the probability (p) for two randomly selected cavities to have overlapping WGM resonances with $Q = 4\times10^3$ is of the order of 1%. In 3D close-pack lattices however each sphere has 12 nearest neighbors that significantly increase the probability of finding resonant WGMs. This probability peaks at wavelengths corresponding to the WGMs in spheres with the mean sizes, as represented by the FL transmission maxima in Figs. 3(a,b). The likely explanation of the observed double peak structure is connected with the well-known property of systems of resonant coupled cavities that form two peaks of the normalized group delay [41-43] at the edges of the transmission band. These peaks provide a distributed feedback for lasing thus explaining why this double peak structure is seen above the lasing threshold.

It should be noted that the regimes of evanescent coupling between the spheres inside such 3D disordered lattices are not well studied at the present time. On the basis of numerical modeling performed for size-mismatched bispheres [18] it can be suggested that the WGM-related transport is undercoupled in the cases with strong detuning between WGM eigenstates. If, however, the detuning is smaller than the on-resonance normal mode splitting [10,15-18]

#88612 - $15.00 USD Received 15 Oct 2007; revised 3 Dec 2007; accepted 4 Dec 2007; published 10 Dec 2007

(~3 nm for 5 μm spheres at the average wavelength 535 nm), one can expect much stronger coupling. More detailed discussion of how the criticality can be achieved in this system can be found in the Conclusions section of this work. In the case of multiple coupled cavities the maximal overlap between their evanescent fields can be achieved if they are located in the same atomic plane of fcc lattice. Within each plane the configurations of well connected clusters of cavities can have an arbitrary shape since their location follows only the principle of minimization of the WGM detuning in a given group of spheres. As an example they can be arranged as sequences of touching cavities with a single path for photons or as clusters of several spheres in a contact. It can be suggested that the formation of a double peak structure in the group delay is generic for different configurations of cavities with nearly resonant WGMs. The physical origin of this phenomenon is connected with the increased dwelling time for photons [41,42] due to multiple back and forth reflections occurring between the cavities at the edges of the CROW pass band. The fact that the amount of splitting between these two peaks does not strongly depend on the spatial arrangement of cavities has been theoretically proven for several different configurations [43] of electronic coupled quantum dots systems. It can be suggested that the optical microcavities should possess similar properties.

In our structures these configurations of cavities with nearly resonant WGMs occupy only a small fraction of volume of the disordered 3D lattice. For this reason these configurations are not visibly contributing to the FL transmission spectra at low pumping intensities. With increasing pumping however, their lasing emission grows stronger than the emission of individual disordered microlasers due to their higher spectral density and competition between the modes. This seems to be the reason why we can observe a spectral signature of coupling between uniform spheres in such disordered 3D lattices. The fact that such clusters of well coupled cavities can be located in different atomic planes of fcc lattice seems to be an important condition for observation of splitting perpendicular to the substrate. As an example in the case of a single monolayer presented in Fig. 2 such photonic molecular states can be formed only in its plane. Using an analogy with the previously observed directional emission of strongly coupled states in resonant bispheres [10] along the axis of bisphere it can be suggested that the molecular states in a single monolayer should be observable rather in the plane of monolayer than in a perpendicular direction.

This interpretation is also consistent with the magnitude of the observed splitting. For multiple cavities it is expected [41] to be higher (by the factor of 2) than the normal mode (WGM) splitting in two identical touching spheres. In this sense the experimentally observed splitting, indicated in Fig. 3 (4.0-5.3nm for 5 μm spheres at the average wavelength 535 nm), is found to be in reasonable agreement with the results of measurements [10,15,17] and modeling [18] of normal mode splitting in polystyrene bispheres with the comparable sizes.

3.3. Thickness dependence of FL transmission

Finally, we studied the dependence of the FL spectral transmission on d using a series of samples with the thicknesses from 9.1 μm (2 monolayers) up to 177 μm (43 monolayers). To enable comparison between the transmission data obtained on different samples we used identical geometries of FL excitation and collection of light, as illustrated in Fig. 4(a) for a six monolayers thick sample. For each sample, the focusing of the pump beam was provided to the area with the same a=30 μm size, whereas the FL transmission was collected from the 10 μm circular area at the back surface of the sample located opposite to the center of the excitation spot. The measurement of the transmitted intensity was complicated by uncontrollable variations in the conditions of excitation and collection of light from sample to sample, leading to ~20% random error in determining the absolute transmitted intensity for different thicknesses (samples). It should be noted however, that the ratio of the intensity of WGM-related peaks to the FL background can be determined for each sample more accurately (few percent error) due to the fact that they are extracted from the same spectrum obtained under identical conditions of excitation and collection of light. It should also be noted, that

#88612 - $15.00 USD Received 15 Oct 2007; revised 3 Dec 2007; accepted 4 Dec 2007; published 10 Dec 2007

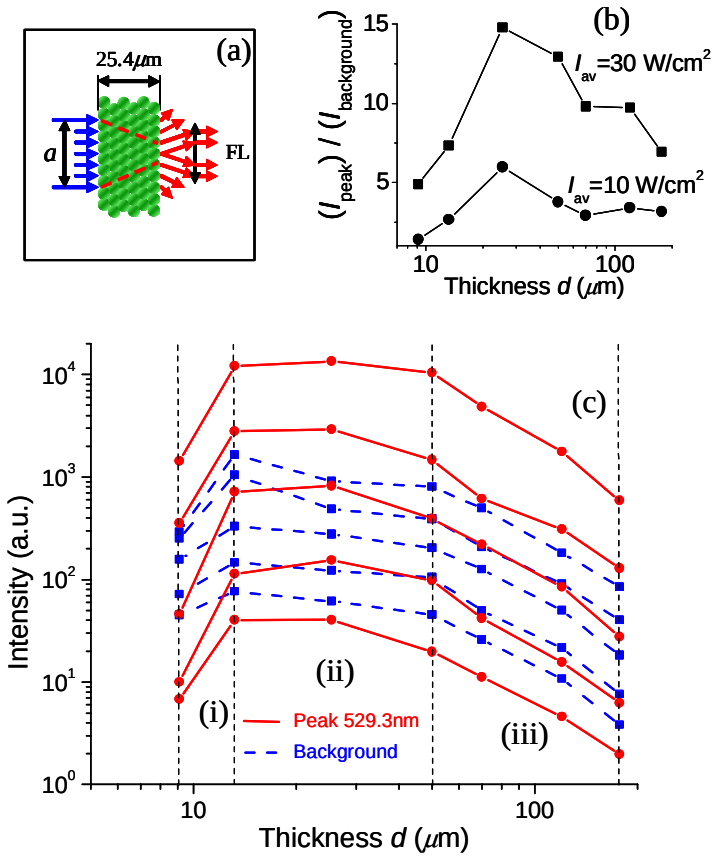

Fig. 4. (a) Geometry of excitation and collection of the FL transmission illustrated for the six monolayers thick sample. (b) Thickness dependence of the peak-to-background ratio at 529.3nm in the FL transmission spectra for two pumping intensities. (c) Thickness dependence of the intensity of the peak at 528nm (red lines) and of the FL background transmission (blue lines). Different curves correspond to excitation intensity from 0.3 W/cm^2 to 30 W/cm^2.

these measurements do not represent the total transmittance [3,4] of the sample because of the limited area (10 μm) and finite angle (20^0) of light collection, but they rather represent its transmission coefficient obtained for many incoming modes (since our FL source is multimode) and for a fixed fraction of transmitted modes.

The results are summarized in Fig. 4(c) for the WGM-related peak at 529.3 nm (red lines) and for the FL background transmission at the same wavelength (blue lines) for various excitation intensities. The thickness dependence can be divided into three regions: (i) two to three layers thick (9.1-13.2 μm) structures where $d \sim l_a$, (ii) intermediate (13.2 μm –50 μm) where $d \sim a > l_a$ and (iii) thick (50 μm-177 μm) structures where $d >> a$, l_a. The regions (i) and (iii) display the dependences which can be qualitatively explained by different factors. The initial increase of the intensities from two to three layers thick structure is explained by more complete absorption of the pump. The decay of the intensities in region (iii) can be explained by the diffusive spread of light generated by the point source.

The results for the intermediate range (ii) of thicknesses in Fig. 4(c) show an anomalous transmission behavior at I_{av}>0.3 W/cm^2, namely the fact that the WGM-related peak at 529.3nm is growing (red lines) as the thickness of the sample increases from d=13.2 μm to d=25.4 μm, whereas the intensity of the FL background is markedly decreased (blue lines) in the same range of thicknesses. This behavior is much better seen in Fig. 4(b) where the peak-

#88612 - $15.00 USD Received 15 Oct 2007; revised 3 Dec 2007; accepted 4 Dec 2007; published 10 Dec 2007

to-background ratio is presented in a linear scale as a function of the thickness of the sample for the two pumping intensities 10 W/cm^2 and 30 W/cm^2. The effect observed at 30 W/cm^2 is quite dramatic with the peak-to-background ratio reaching the maximum for the 25.4 μm sample where it significantly exceeds this ratio for other samples with different thicknesses. This result cannot be explained simply by more complete absorption of the pump in the 25.4 μm sample since the FL background transmission (which should depend on the absorption of the pump in a similar way) is markedly decreased in the 25.4 μm sample compared to the thinner 13.2 μm sample. By translating the sample in the direction perpendicular to the optical axis of the set-up, we found that the magnitude of this effect is positional dependent. This can be related to the polycrystalline structure of our samples. Despite its varying magnitude this effect was present in most of the areas of the sample. It should also be noted that this effect takes place not for all, but only for some of the WGM-related peaks.

The interpretation of this effect is related to the mechanism of the WGM-related transport. Since the FL background propagates diffusively, as it was discussed in Section 3.2, the strong peak-to-background ratio observed in samples with the thickness 25.4 μm means that the WGM-related transport tends to be more efficient than classical diffusion of light for such thicknesses. One of the possible interpretations of this result is connected with the assumption that the WGM-related lasing occurring in the thin, near-surface layer of the structure is highly directional along the normal to the surface of the sample. This assumption however, is not supported by our observations of the spatial distribution of the FL transmission as a function of pumping which demonstrated a broad (>60^0) angular spread of the transmitted modes. A more likely explanation of this effect is connected with the presence of clusters of nearly resonant spheres stretching from one side to the opposite side of the structure. These clusters can play the role of very efficient waveguides for WGM transport. The termination of these waveguides at the back surface of the structure (or inside the structure) leads to a strong scattering thus explaining the broad angular distribution of the transmitted modes. The decreased peak-to-background ratio observed in thicker (d≥50 μm) samples, as illustrated in Fig. 4(b), can be explained in this model by the fact that the characteristic sizes of the connected clusters are much smaller than the thicknesses of the samples that should lead to diffusive mechanism of light transport.

4. Conclusions

In conclusion, using techniques of flow-assisted self-assembly, we synthesized 3D lattices of microspheres with the well controllable thickness from one monolayer up to 43 monolayers of closed packed spherical cavities. In the low-intensity (I_{av}<0.3 W/cm^2) FL transmission spectra of such 3D lattices, we observed a series of nearly equidistant maxima determined by the inhomogeneous broadening of WGM resonances in the individual size-disordered spheres. With increasing pumping intensities (I_{av}>0.3 W/cm^2), we observed that each maximum splits into a double-peak structure which can be associated with two peaks of normalized group delay well-known [41-43] for systems of resonant cavities. This effect was explained by the presence of clusters of spheres with close positions of their WGM resonances inside our disordered 3D lattices which can be more efficiently excited at high pumping powers. In the thickness dependence of the FL transmission spectra it was observed that the ratio of the intensity of some of the WGM-related peaks to the FL background can be anomalously high for samples with the thickness around 20-30 μm. This effect was explained by the presence of clusters of spheres with typical sizes 20-30 μm which are well connected at the WGM wavelengths providing more efficient transport through the structure.

In this paper we developed an approach to understanding the optical transport properties of such systems based on the analogy with the bond percolation problem [31-33] in percolation theory. In this approach, the lattice sites (spheres) are connected with optical “bonds” that are present with probability p depending on the cavities’ size dispersion (assuming p≈1 in the case of resonance between WGMs). Due to a 3% size disorder, the structures studied in this work with Q = 4×10^3 are characterized with p~0.01, thus only small clusters of sites connected by

#88612 - $15.00 USD Received 15 Oct 2007; revised 3 Dec 2007; accepted 4 Dec 2007; published 10 Dec 2007

bonds can form. However, by selecting more uniform spheres it should be possible to reach a percolation threshold (p_c = 0.1201635 for an fcc lattice [32]) where a giant cluster spans the entire network. It should be noted that in the case of WGM coupling in 3D case the multiple spheres can be preferably connected in the "atomic" plans of such fcc lattice that should result in anisotropic properties and higher than p_c=0.1201635 thresholds of such percolative transport, however still the WGM transport in a 3D lattice of spheres is expected to be much more robust to the presence of disorder compared to that in 1D chains or 2D arrays of cavities. Above the percolation threshold such lattices should become transparent for the WGM transport irrespective of the sample thickness. In comparison with single chains of cavities, 3D structures operating above the WGM percolation threshold can tolerate an order of magnitude larger dispersion of spheres sizes.

The level of uniformity of spheres required for achieving such WGM percolation threshold depends on their mean size since smaller spheres have smaller *Q*-factors of their WGM resonances which are easier to overlap. We predict that the WGM percolation threshold should be achievable in close packed 3D lattices formed by cavities with Q~10^3 and with ~1% size dispersion. As an example this situation can be realized using commercially available ~3 μm polystyrene spheres in air. The notion of criticality, however, is lost in this case since the resonators are overcoupled due to the fact that the normal mode splitting exceeds the uncoupled WGM linewidths. It is interesting to note that there is an additional parameter for designing such structures which in principle allows achieving regime of critical coupling under conditions of percolative transport. This parameter is represented by the index of the external medium. As an example similar values of Q~10^3 with ~1% size dispersion can be realized using enlarged (~10 μm) polystyrene spheres in water. In the same spectral range WGMs in these spheres are characterized with larger angular (l) numbers compared to 3 μm spheres. On the other hand, as it was demonstrated [21] by using numerical modeling, the modes with larger l numbers are characterized with smaller coupling constant (and normal mode splitting) due to smaller fraction of the evanescent field outside the cavity. This effect was found to be very dramatic [21] for the cylindrical cavities where the change of l from 10 to 16 reduced the coupling constant by approximately five times. On the basis of these results it seems feasible to achieve critical coupling of enlarged spheres (~10 μm) in a liquid environment. The exact parameters of spheres and liquid medium should be identified through numerical modeling that will be the subject of our future work. Such structures of critically coupled cavities with percolative WGM transport can be used for multi wavelength detection of biochemical-binding events at the liquid-sphere interface. Thus, such systems can be used for developing next generation of resonant sensors and arrayed-resonator light emitting devices.

Acknowledgments

The authors thank M.S. Skolnick, M. Sumetsky, J.J. Baumberg, M.A. Fiddy and M.E. Raikh for stimulating discussions. This work was supported by ARO grant W911NF-05-1-0529 and by NSF grant CCF-0513179 as well as, in part, by funds provided by the University of North Carolina at Charlotte. S.P. Ashili was supported by DARPA grant W911NF-05-2-0053. The authors are thankful to Duke Scientific Corporation for donating microspheres for the research presented in this work.

#88612 - $15.00 USD Received 15 Oct 2007; revised 3 Dec 2007; accepted 4 Dec 2007; published 10 Dec 2007